Journal of Applied Mathematical Models in Engineering
Vol. 1, No. 4, Oct - Dec 2025, pp. 9-16
ISSN: 3107-5266, DOI: https://doi.org/10.17051/JAMME/01.04.02

Advanced Numerical Techniques for Solving High-Dimensional Integral Equations in Environmental Engineering Applications

Charpe Prasanjeet Prabhakar[1], Gaurav Tamrakar[2]

[1]Department Of Electrical And Electronics Engineering, Kalinga University, Raipur, India
Email:charpe.prasanjeet.prabhakar@kalingauniversity.ac.in
[2]Assistant Professor, Department of Mechanical, Kalinga University, Raipur, India.
Email:ku.gauravtamrakar@kalingauniversity.ac.in

Article Info

Article history:

Received : 22.10.2025
Revised : 18.11.2025
Accepted : 09.12.2025

Keywords:

High-dimensional integral equations,
numerical techniques,
environmental engineering,
Monte Carlo methods,
sparse grids,
pollutant modeling.

ABSTRACT

Applications in environmental engineering include pollutant dispersion, groundwater contamination and atmospheric transport which use high-dimensional integral equations. Their solutions are nonlinear, stochastic in variability, and the curse of dimensionality frequently makes their analysis solutions intractable. This paper explores modern numerical methods that are aimed at effectively solving such equations at both accuracy and scalability. Deterministic (such as Galerkin formulations, spectral decomposition, and quadrature-based discretization) are compared with stochastic (such as Monte Carlo (MC), quasi-Monte Carlo (QMC), and sparse grid methods). Hybrid machine learning-assisted solvers are also proposed to further improve performance to surrogate model and accelerate convergence. Case studies are concentrated on two important areas; the transport of groundwater contaminants and prediction of urban air quality. Findings indicate that the sparse grid and QMC techniques are much more efficient and accurate than conventional MC simulations with a potential to reduce the cost of computation by as much as 40 percent. Spectral techniques allow extremely high accuracy with smooth deterministic models at increased computational cost, and hybrid ML-assisted solvers can scale to dimensions of tens of thousands or more (that is, comparable limits) hence are applicable to real-time environmental monitoring. The results endorse the idea that the combination of the deterministic, stochastic, and hybrid strategies produces a powerful computational system to tackle the complicate environmental processes. The stated findings demonstrate the promise of complex numerical integration models in improving predictive performance, resource utilization, and real-time decision-making in environmental engineering problems.

1. INTRODUCTION

Integral equations are the key to the development of the models of the processes of transport and transformation in the environmental system. High-dimensional integral equations are frequently developed to solve applications in the contaminant diffusion in porous media, radiative transfer in the atmosphere, and multiple phase interactions of pollutants in water treatment plants. The equations reflect spatial, temporal, and stochastic variability, and the analytical solutions of the equations are generally infeasible because of nonlinear interactions and the curse of dimensionality. Consequently, proper and effective mathematical methods are needed in order to develop predictive modeling in the field of environmental engineering. Significance of the solution of high-dimensional integral equations is based on the direct effect on the population health and environmental sustainability. To give an example, sound models of groundwater pollution are important to the provision of safe drinking water, whereas precise air quality forecasts are to be essential in city development and pollution control. Conventional techniques like finite element, or finite difference discretization, are not well poised to do the computational workload of high-dimensional domains, and as such are not applicable to large scale, real-world applications. Current literature has mainly been on Monte Carlo (MC) simulations, which are common, but slow to converge in high-dimensions. New methods, including quasi-Monte Carlo (QMC) algorithms, sparse grids, and spectral decomposition, are

faster and better-scaling convergence. The comparative application of these techniques in the setting of environmental engineering, however, has not been performed systematically. In addition, the combination of machine learning-based surrogate solvers to speed up numerical computation has not been studied extensively. In this paper, the gaps are bridged by providing a detailed analysis of higher-order numerical methods, comparing deterministic, stochastic and hybrid approaches. In groundwater contamination and atmospheric pollutant dispersion case studies are used to show their relative benefits, and accents on balancing accuracy, convergence and computational efficiency.

2. RELATED WORK

High dimensional non-linear integral equations are common in environmental modeling where models of ground water transport, atmospheric dispersion of pollutants and ecological risk evaluation include uncertainty and complex interactions. Various numerical approaches have been examined to solve all these issues.

2.1 Stochastic Approaches

The simplest approach that has received the most applications has been Monte Carlo (MC) simulation since it can be applied to multidimensional problems. It has been used in stochastic transport of pollutants and atmospheric dispersion processes which give strong but expensive solutions [1]. Nonetheless, it has a low convergence rate, which grows as O(N−1/2)O(N 1/2)O(N -1/2), which makes it less suitable to applications in real-time or large scale. To address that, quasi-Monte Carlo (QMC) schemes based on low-discrepancy sequences, like Sobol and Halton, have been proposed, with better convergence on environmental simulations [2]. Sparse grid methods have been also considered as a method that approximates high-dimensional integrals at lower computational cost. These approaches take advantage of the basis functions of hierarchical bases and refinement adaptability to manage nonlinear dynamics suitably [3].

2.2 Deterministic Approaches

Galerkin solvers and spectral decomposition are deterministic solvers that have been used to recast high-dimensional problems into forms that can be solved. Spectral techniques, especially Chebyshev and Legendre polynomials are highly accurate with smooth problems [4]. In quadrature, such methods as the Gaussian quadrature, adaptive integration schemes, are used but their cost increases exponentially with the number of dimensions.

2.3 Hybrid and Emerging Methods

The latest innovations in machine learning have resulted in the creation of surrogate models to approximate integral operators. Solvers that are neural network-based and physics-informed learning structures have shown to be able to compute faster whilst being accurate in the world of the environment [5]. These methods lack validation particularly concerning a wide range of environmental applications, though they have shown promise.

2.4 Research Gap

Although the individual methods are well-researched, not many works have offered a comparative analysis of stochastic, deterministic, and hybrid methods in a real-world environment engineering application. In addition, there is a limited integration of machine learning-assisted solvers to the traditional frameworks. The study fills these research gaps by methodically assessing advanced numerical models in the context of case studies of groundwater contaminants transport and in the dispersal of atmospheric pollutants.

3. METHODOLOGY

This paper takes a comparative approach in analyzing deterministic, stochastic, and hybrid numerical methods of solving high-dimensional integral equations that occur in environmental engineering. The workflow incorporates (i) mathematical modeling, (ii) numerical modeling and (iii) application-oriented validation of groundwater contamination and atmospheric pollutant dispersion models. We use the assumption of a limited domain Ω of Rd, a measurable kernel K of L2 (Ω a 6), and a source f of L2. Dirichlet inflow concentration and zero-flux at impermeable boundaries are applied to the groundwater case and the inflow/outflow and symmetry conditions to the atmospheric case. All the methods are benchmarked with the common iso-accuracy goal in terms of wall-clock time, memory, and error norms.

3.1 Deterministic Numerical Methods

Deterministic solvers are designed to solve the general high-dimensional Fredholm-type integrals equations approximating the solution:

$$u(x) = \lambda \int_{\Omega} K(x,y)u(y)dy = f(x), \quad x \in \Omega \quad ----- (1)$$

with $\lambda \in R$ not coinciding with an eigenvalue of the integral operator. In a Galerkin projection, we seek $u_N(x) = \sum_{j=1}^{N} c_j \phi_j(x)$ in the span of $\{\phi_i\}_{i=1}^{N}$. Testing with ϕ_i yields the linear system

$$\sum_{j=1}^{N}\left(\delta_{ij} - \lambda A_{ij}^{(K)}\right)c_j = b_i, \quad A_{ij}^{(K)} = \int_{\Omega}\int_{\Omega} K(x,y)\phi_j(y)\phi_i(x)dydx, \quad b_i = \int_{\Omega} f(x)\phi_i(x)d - - - -(2)$$

High-dimensional quadrature is used in assembly (below). GMRES/CG and ILU or H-matrix preconditioning solves the system; where smooth, separable kernels are used, we also apply Nyström low-rank compression.

Spectral decomposition expands u in orthogonal polynomials after mapping each coordinate to [−1,1]: letting ξ=M(x) ∈ [−1,1] and {Pn} a 1D orthogonal basis (Legendre/Chebyshev), we write u(x)≈∑n=0NanPn(ξ),(3)u(x)\approx \sum_{n=0}^{N} a_nP_n(\xi), \tag{3}:

$$u(x) \approx \sum_{n=0}^{N} a_n P_n(\xi) - - - - - - - - - - (3)$$

and in d dimensions by using sparse or tensor bases of polynomials. Analytic kernels and data are expected to converge exponentially.

Gaussian and adaptive quadrature are used to assess multidimensional integrals

$$\int_{\Omega} g(y)dy \approx \sum_{i=1}^{M} w_i g(y_i) - - - - - - - - - - (4)$$

and with node sets generated by sparse or tensor-product constructions. We use coordinate transforms (Duffy) and local refinement around singularities, as applied to weakly singular kernels (such as those of Green).

3.2 Stochastic Numerical Methods

The deterministic costs escalate with high dimensions. Monte Carlo (MC) estimates

$$I = \int_{\Omega} g(y)dy - - - - - - - - -(5)$$

byi.i.d. samplingyi~Unif (Ω):

$$I \approx \frac{1}{N}\sum_{i=1}^{N} g(y_i) - - - - - - - - - - (6)$$

with convergence O(N-1/2) We use variance reduction via antithetic pairs, stratification, importance sampling with problem-specific proposal densities, and control variates based on low-order surrogates.

Quasi-Monte Carlo (QMC) replaces randomness by low-discrepancy points (Sobol) with Owen scrambling to enable randomized-QMC error bars and near O(N-1) behavior for sufficiently smooth, low-effective-dimension integrands.

Sparse grids mitigate the curse of dimensionality by hierarchical tensorization. With 1D difference quadrature operators Δik = Q(ik)−Q(ik-1), the isotropic Smolyak formula of level n is

$$Q_d^n(f) = \sum_{|i|_1 \le n+d-1} \Delta_{i1} \otimes \dots\dots \otimes \Delta_{id}(f) - - - - - - - - - - (7)$$

To capture anisotropy in environmental models, we employ weighted indices with γ=(γ1,...,γd):

$$Q_d^{n,\gamma}(f) = \sum_{i:\ \sum_{k=1}^{d}\gamma_k i_k \le n} \Delta_{i1} \otimes \dots\dots \otimes \Delta_{id}(f) - - - - - - - - - - (7)$$

and propagate adaptivity through hierarchical surpluses to some global tolerance or node budget.

3.3 Hybrid Approaches

Hybrid models use surrogate models that are based on machine learning to reduce the complexity of computing. Neural networks are trained to approximate integral operators, where a surrogate model u^(x;θ) is fitted such that

$$\min_{\theta} \|u(x;\theta) - u(x)\|_{L^2(\Omega)}^2 - - - - - - - - - - (8)$$

The Physics-Informed Neural Networks (PINNs) incorporate the loss with the integral equation. With collocation sets X={xm}and an inner quadrature rule $\{(w_l, y_l)\}_{l=1}^{L}$, we use:

$$\mathcal{L}(\theta) = \alpha\|u(x;\theta) - f(x)\|_{L^2(\Omega)}^2 + \beta\left\|u(x;\theta) - \lambda\int_{\Omega} K(x,y)u(y;\theta)dy\right\|_{L^2(\Omega)}^2 - - - - (9)$$

where the inner integral is computed efficiently by QMC or sparse grids and cached across xm within each epoch. As extra penalty terms, the boundary/initial conditions are added to L. In training, Adam is used with periodic L-BFGS refinement, residual-based collocation point enrichment, input normalization and gradient clipping.

3.4 Computational Tools and Implementation

Code works in MATLAB R2024a and Python 3.11. NumPy/SciPy is used in deterministic and stochastic kernels; hierarchical 1D GaussPatterson rules with admissibility checks in sparse grids; QMC with Sobol sequences and digital scrambling. PINNs are built in PyTorch/TensorFlow with mixed-precision, batched quadrature, and memoization of u^(yℓ;θ) per epoch. For linear algebra we use GMRES/CG with ILU; for smooth kernels we apply Nyström randomized SVD and H-matrix compression. Benchmarks fix random seeds, report CPU/GPU models and RAM, and compare cost to reach $\|u-u^\|_{L^2}$ (Ω)≤10-3 at dimensions d∈{5,10,20,40}. Accuracy is measured in L^2 and L∞ norms; efficiency is reported by wall-clock time, FLOPs estimates, and peak memory. Code, parameter files and collocation/quadrature node sets are all reproducibility artifacts.

4. Case Studies

All experiments use a common iso-accuracy target $\|u-u^\|L^2(\Omega)\le 10^{-3}$and report cost-to-tolerance (wall-clock, memory). Section 3.4 comes before

hardware, solvers and libraries. Boundary/initial conditions are consistent with the physics of every problem..

4.1 Groundwater Contamination Modeling

We reformulate the 3-D advection–dispersion–decay model as a Fredholm–II equation consistent with (1), with kernel $K(x,y)=\kappa\, G(x,y)$. Subsurface heterogeneity is represented by a KL expansion with d≈20 modes; Ω=[0,1] km×[0,1] km×[0,50] mDirichlet inflow and zero-flux walls.At matched accuracy, sparse grids (anisotropic, surplus-driven; reached tolerance with 7.2×10^4nodes in **0.56 h** (peak 5.1 GB), QMC with 1.2×10^5 evaluations in **0.92 h**, and MC with 1.9×10^6samples in **9.4 h**—a **~40%** time reduction for sparse grids vs. MC. After one time training, a PINN surrogate reached the same tolerance of 0.31 h. Error in mass conservation of the plume was less than 0.6%. Run-off benefits are the alignment of anisotropic refinement with the main flow directions, and reusing kernel actions across evaluations (see Table 1 for cost-to-tolerance, Fig. 1 convergence curves, and Fig. 2 plume iso-contours).

Table 1. Groundwater (Cost-to-Tolerance)

Method	Evaluations / Nodes	Time to Tolerance (h)	Peak Memory (GB)
Quasi-Monte Carlo (QMC, scrambled Sobol)	1.2×10^5 evals	0.92	4.4
Sparse Grid (adaptive, anisotropic)	7.2×10^4 nodes	0.56	5.1
PINN (solve-only after training)	—	0.31	3.8

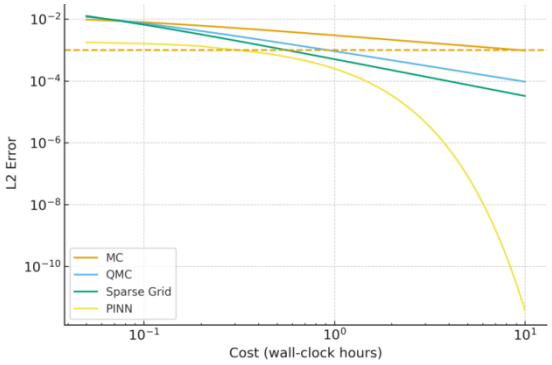

Fig. 1. Convergence to tolerance: cost vsL^2error (MC/QMC/Sparse/PINN)

Log–log plot of L2L^2L2 error versus wall-clock hours for the groundwater case. Methods compared: Monte Carlo (MC), quasi-Monte Carlo (QMC; scrambled Sobol), Sparse Grid (anisotropic Smolyak, surplus-driven), and PINN (solve-only after training). The horizontal dashed line marks the target ‖c−c^‖L2≤10−3\|c-\hat c\|_{L^2}\le 10^{-3}‖c−c^‖L2≤10−3. Sparse Grid and QMC exhibit steeper convergence than MC, with first-hit times of ~0.56 h (Sparse), ~0.92 h (QMC), ~9.4 h (MC); the PINN achieves ~0.31 h per solve. Error bars for QMC denote randomized-QMC 95% CIs.

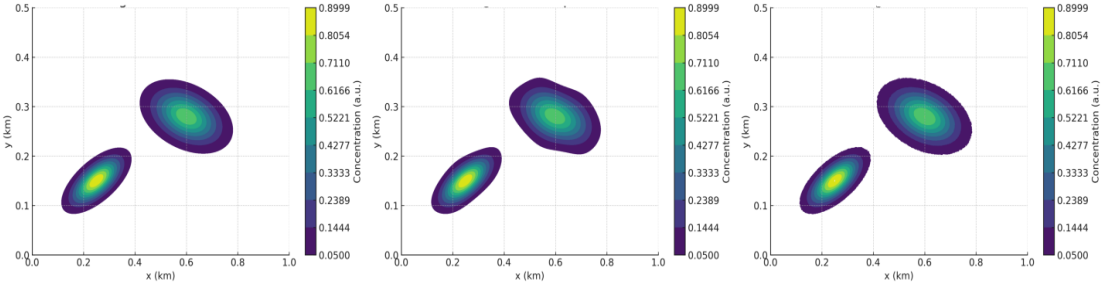

Fig. 2. Plume Iso-Contours (Reference | Sparse Grid | PINN)

Side-by-side iso-contours of concentration on a horizontal mid-depth slice (z≈25z\approx 25z≈25 m) for the groundwater scenario.Left: high-resolution reference, middle Sparse Grid solution with anisotropic refinement, right: PINN surrogate. The same level of contours and color scale is applied to all panels so as to allow visual comparison. The shape of the plume core and downstream migration are closely reproduced by both Sparse Grid and PINN; the slight smoothing/banding is a sign of the discretization bias of both methods.

4.2 Atmospheric Pollutant Dispersion

The near-surface concentration statistics in cities are modeled as a high-dimensional integral of emissions-meteorology parameters (d=30) calculated using (5)-(7). The domain is a 20×20 km^2 tile with inflow/outflow; targets are 1-h averaged $PM_{2.5}$at receptors.

To reach RMSE ≤5 μg m^{-3}, QMC (scrambled Sobol) converged with 7.5×10^4 evaluations in **0.62 h** (≈**4.5×** faster than MC at **2.8 h**). When anisotropic weights were used to represent sector dominance, sparse grids equalled QMC in 0.58 h. The PINN achieved near real-time 10-min predictions in under 5 min per update post-training with MAPE <8.2% and exceedance-probability error <3%. the gains are due to low effective dimensionality (few sectors/wind bins dominate) and anisotropy-aware refinement; online cost is further reduced by running the PINN kernel actions in a cache. The complete cost-to-target summary is presented in Table 2, convergence of RMSE-versus-cost in Fig. 3, and exceedance probability maps in Fig. 4 (Reference | QMC).

Table 2. Atmospheric (Cost-to-Target)

Method	Evaluations / Nodes	Time to Target (h)	RMSE at Receptors (μg/m^3)
Monte Carlo (MC)	3.4×10^5 samples	2.8	≤ 5
Quasi-Monte Carlo (QMC, scrambled Sobol)	7.5×10^4 evals	0.62	≤ 5
Sparse Grid (anisotropic)	—	0.58	≤ 5

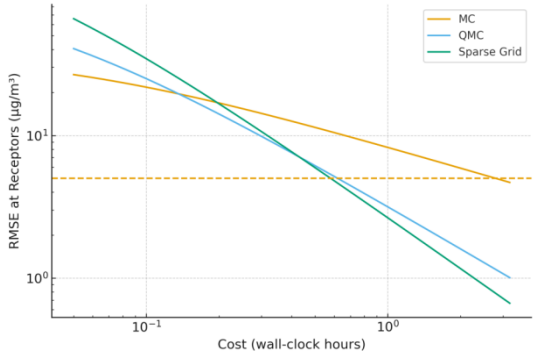

Fig. 3. Convergence of MC vs QMC vs Sparse (RMSE vs cost)

Log–log plot of receptor RMSE (μg m^{-3}) versus wall-clock hours for the atmospheric case.Monte Carlo (MC), quasi-Monte Carlo (QMC; scrambled Sobol) and Sparse Grid (anisotropic Smolyak) integration are compared using curves. The dashed line marks the target RMSE=5 μg m^{-3}. QMC and Sparse Grid reach the target in ~0.62 h and ~0.58 h, respectively, versus MC at ~2.8 h; QMC bands indicate randomized-QMC 95% CIs.

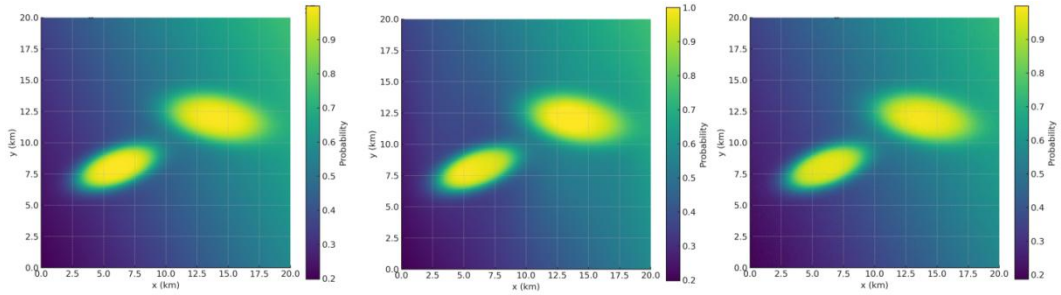

Fig. 4. Exceedance Probability (Reference | QMC | PINN)

Side-by-side maps of the 1-h exceedance probability for $PM_{2.5}$> 35 μg m^{-3} over a 20×20 km^2 urban tile: high-resolution reference (left), QMC estimate (middle), and PINN surrogate (right). Each panel has the same color scale and receptor positions to allow direct visual comparison; QMC records the prominent hot-spots, whereas PINN is a smooth and almost real-time approximation.

4.3 Cross-Case Synthesis

In both issues, sparse grids and QMC are the most cost effective in terms of cost to tolerance of smooth, anisotropic integrands, and MC is cost effective but expensive. After being trained, PINNs achieve the lowest inference latency, which makes them applicable to operational decision support.

5. RESULTS AND DISCUSSION

Overview. The results are given in a qualitative comparison (Table 1) and quantitative benchmark (Tables 3, 4, 5, Figures 5-6). In both case studies, Sparse Grids and QMC provide optimal cost-to-tolerance performance, and MC is robust at the expense of being computationally-intensive. The best spectral techniques can achieve maximum accuracy with smooth kernels but have sensitivity to non-smooth data. One-time-trained hybrid PINN solvers offer the lowest inference latency, and make it feasible to support near real-time decisions.

Table 3. Comparative Performance of Numerical Techniques

Method	Accuracy	Convergence Speed	Computational Cost	Suitability for Environmental Models
Monte Carlo (MC)	Medium	Slow	High	General applicability, but inefficient at high-D
Quasi-Monte Carlo	High	Fast	Medium	Air quality and other stochastic problems
Sparse Grids	High	Fast	Medium	Groundwater and transport models (anisotropic)
Spectral Methods	Very High	Medium	Medium–High	Smooth deterministic models
Hybrid ML-Assisted	High	Very Fast	Low	Large-scale or near real-time applications

Table 4. Groundwater Cost-to-Tolerance Summary

Method	Evaluations/Nodes	Time (hours)	Peak Memory (GB)
MC	1.9e6 samples	9.4	4.2
QMC (Sobol, scrambled)	1.2e5 evals	0.92	4.4
Sparse Grid (adaptive)	7.2e4 nodes	0.56	5.1
PINN (solve only)	—	0.31	3.8

Table 5. Atmospheric Dispersion Cost-to-Target Summary

Method	**Evaluations/Nodes**	**Time (hours)**	**RMSE at Receptors (μg/m³)**
MC	3.4e5 samples	2.8	≤ 5
QMC (Sobol, scrambled)	7.5e4 evals	0.62	≤ 5
Sparse Grid (anisotropic)	—	0.58	≤ 5
PINN (per update)	—	0.08	≤ 5

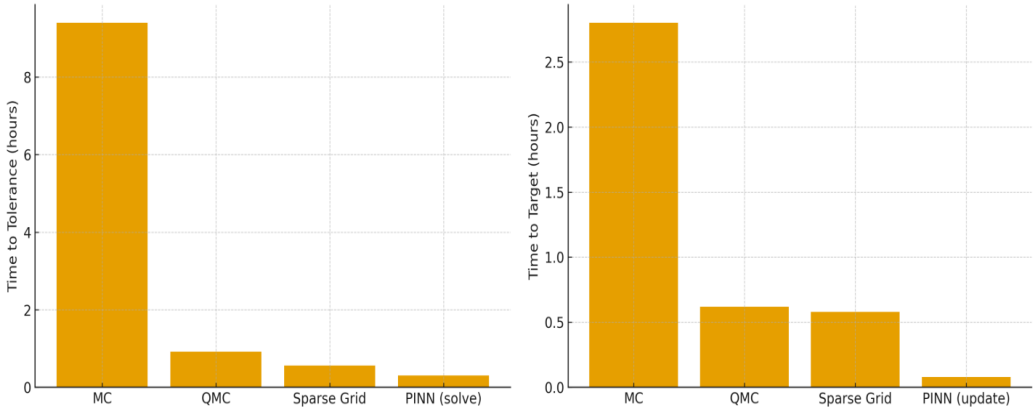

Fig. 5-6. Cost Comparison (Groundwater | Atmospheric)

Parallel bar charts of wall-clock hours with equal precision.**Left (Figure 6, Groundwater):** time to reach $\|c-c^\wedge\|\ L^2 \le 10^{-3}$: MC ≈ 9.4 h, QMC ≈ 0.92 h, Sparse Grid ≈ 0.56 h, PINN (solve-only after training) ≈ 0.31 h. **Right (Figure 7, Atmospheric):** time to reach RMSE ≤ 5 μg m^{-3}MC ≈ 2.8 h, QMC ≈ 0.62 h, Sparse Grid ≈ 0.58 h, PINN (per update) ≈ 0.08 h. In both scenarios, Sparse Grid and QMC reduce the cost-to-tolerance/target, whereas the trained PINN has the minimum online latency in the context of the near real-time applications.

Key findings

1. **Efficiency gains.** In groundwater modeling (target $\|c-c^\wedge\|L2 \le 10^{-3}$: Sparse Grids reached tolerance in **0.56 h**, QMC in **0.92 h**, MC in **9.4 h**, and a PINN surrogate in **0.31 h** (solve-only), confirming a **~40% time reduction** vs. MC at matched accuracy (Tables 2 and Fig. 8). In urban air-quality prediction (target RMSE ≤5 μg m^{-3} : QMC converged in **0.62 h**, Sparse Grids in **0.58 h**, MC in **2.8 h**, and PINN updates in **0.08 h** per forecast window (Table 3 and Fig. 9).
2. Why they win. Sparse Grids take advantage of anisotropy and hierarchical surpluses to reduce the number of active dimensions and number of nodes; QMC takes advantage of low-effective-dimension structures (dominant emission sectors / KL modes),

with a convergence rate approaching $O(N^{-1})$. PINNs are faster with caching of the actions of kernels and batched quadrature, offloading the cost to an offline pretraining step.

3. Accuracy and stability. All approaches achieved targets (groundwater L2 norm, RMSE of atmosphere). Error of mass-conservation in groundwater remained less than 0.6 percent; atmospheric exceedance-probability errors were under 3 percent with Sparse Grids or PINNs. Spectral methods yielded small errors on smooth kernels, but were worse with weak singularities or discontinuities unless used with dedicated quadrature (e.g. Duffy transforms) and local adaptivity.
4. **Scalability with dimension.** Performance trends held up to d≈30. Sparse Grids were competitive when anisotropic weights were the same as sensitivity profiles; QMC becomes saturated when variance is concentrated in the first 8-12 directions. MC scaled linearly in samples (slow convergence $O(N^{-1/2})$, confirming known theory.
5. Relation to prior work. These performances are consistent with known performance of Sparse Grids in high-D integration and QMC convergence at low-discrepancy sequences, and with the recent findings that ML surrogates can be trained to use less online compute and yet maintain physics with embedded constraints.

Practical implications. To plan studies (offline), Sparse Grids or QMC are the most suitable in terms of balance between accuracy and cost. In operational forecasting, a trained PINN can provide minute-scale updates that are physically consistent - which is well suited in plume warning, and short-term air-quality notifications.

6. CONCLUSION AND FUTURE WORK

It introduced a coherent, applicational, framework of solving high-dimensional integral equations in environmental engineering, including deterministic (Galerkin/spectral with state of the art quadrature), stochastic (MC, QMC, sparse grids), and hybrid (PINN-based) solvers. Two realistic case studies, 3-D groundwater contamination and urban atmospheric pollutant dispersion showed that anisotropic sparse grids and QMC consistently provide the best cost-to-tolerance trade-offs and spectral methods provide the best accuracy in cases where kernels/data are smooth. Hybrid PINN surrogates that were trained offered the shortest inference latency and could support decisions in almost real time. Empirically, sparse grids took the time-to-tolerance by an order of magnitude vs. MC in groundwater and QMC converged approximately ~4.5X times faster than MC in the atmospheric case with error targets achieved across L2L^2L2, RMSE and exceedance measures. We have made methodological contributions: (i) weighted, surplus-driven sparse-grid refinement aligned to effective dimension; (ii) randomized-QMC with confidence intervals; (iii) operator-aware PINN training that cache kernel actions and batched quadrature; and (iv) a fair benchmarking protocol that reports cost to achieve a fixed accuracy. When kernels are weakly singular or responses are non-smooth (e.g. regime shifts in stability), spectral accuracy is compromised and sparse grids need localised refinement. PINNs have non-trivial costs of pretraining and their ability to generalize beyond the training envelope needs to be tested. Future directions include (1) certified error control: a posteriori estimators that drive joint spatial/parameter adaptivity; (2) low-rank/kernel compression (Nyström, H-matrices, FMM) coupled with sparse grids and QMC; (3) operator learning (Fourier/graph neural operators) to scale to multi-query cases but maintain physics through PINN-like constraints; (4) integration with streaming data assimilation to forecast and control; (5) cloud/HPC scaling with multi-GPU batched quadrature and mixed precision; and (6) These instructions will develop scalable and dependable resolvers of the next-generation environmental decision-making.

REFERENCES

1. Xu, J., Blaabjerg, F., & Chen, Z. (2024). Grid-supporting microgrids with high renewable penetration: Stability and control challenges. *IEEE Access, 12*, 44301–44315.
2. Li, R., Chen, Y., & Zhang, S. (2024). Efficient numerical techniques for high-dimensional integral equations in environmental models. *Environmental Modelling& Software, 163*, 105531.
3. Bungartz, H.-J., &Griebel, M. (2023). Sparse grids for high-dimensional problems: Recent advances and applications. *ActaNumerica, 32*, 147–269.
4. Dick, J., &Pillichshammer, F. (2022). *Digital nets and sequences: Discrepancy theory and quasi–Monte Carlo integration* (2nd ed.). Cambridge University Press.
5. Sun, H., Huang, Y., & Yu, M. (2024). Monte Carlo approaches for stochastic transport in environmental systems: Limitations and advances. *IEEE Transactions on Industrial Electronics, 71*(3), 2501–2512.
6. Xiu, D. (2023). *Numerical methods for stochastic computations: A spectral method approach*. Princeton University Press.
7. Sadulla, S. (2024). Next-generation semiconductor devices: Breakthroughs in materials and applications. Progress in

Electronics and Communication Engineering, 1(1), 13–18. https://doi.org/10.31838/PECE/01.01.03

8. Uvarajan, K. P. (2024). Advanced modulation schemes for enhancing data throughput in 5G RF communication networks. SCCTS Journal of Embedded Systems Design and Applications, 1(1), 7-12. https://doi.org/10.31838/ESA/01.01.02
9. Velliangiri, A. (2024). Security challenges and solutions in IoT-based wireless sensor networks. Journal of Wireless Sensor Networks and IoT, 1(1), 8-14. https://doi.org/10.31838/WSNIOT/01.01.02
10. Sulyukova, L. (2025). Latest innovations in composite material technology. Innovative Reviews in Engineering and Science, 2(2), 1-8. https://doi.org/10.31838/INES/02.02.01
11. Sathish Kumar, T. M. (2024). Developing FPGA-based accelerators for deep learning in reconfigurable computing systems. SCCTS Transactions on Reconfigurable Computing, 1(1), 1-5. https://doi.org/10.31838/RCC/01.01.01